Am J Cancer Res 2022;12(11):5300-5314
www.ajcr.us /ISSN:2156-6976/ajcr0145732

Original Article

Identification of BIK as an unfavorable prognostic marker and novel therapeutic target in microsatellite stable colorectal cancer harboring KRAS mutations

Peng Liu[1*], Feng Jiao[2*], Zhenghua Zhang[3*], Feilong Zhao[4], Jinping Cai[4], Shiqing Chen[4], Tao Fu[5], Min Li[6]

[1]Department of Colorectal Surgery, Changhai Hospital, Naval Medical University, Shanghai, China; [2]Department of Oncology, Renji Hospital, School of Medicine, Shanghai Jiaotong University, Shanghai, China; [3]Department of Oncology, Jing'an District Centre Hospital of Shanghai, Huashan Hospital Fudan University Jing'an Branch, Shanghai, China; [4]Medical Affairs, 3D Medicines, Inc., Shanghai, China; [5]Department of Gastrointestinal Surgery, China-Japan Friendship Hospital, Beijing, China; [6]Department of Oncology, Nanjing Hospital of Chinese Medicine Affiliated to Nanjing University of Chinese Medicine, Nanjing, Jiangsu, China. [*]Equal contributors.

Received August 3, 2022; Accepted October 14, 2022; Epub November 15, 2022; Published November 30, 2022

Abstract: *KRAS* mutations lead to persistent activation of multiple downstream effectors that drive the cancer phenotype. Approximately 30%-50% of colorectal cancer (CRC) patients harbor *KRAS* mutations, which confer more aggressive tumor biology and shorter overall survival (OS), especially in microsatellite stable (MSS) metastatic CRC. Given that KRAS mutant protein has been proven difficult to target directly, identifying genes that function closely with *KRAS* and targeting these genes seems to be a promising therapeutic strategy for *KRAS*-mutated MSS CRC. Here, *KRAS* function-sensitive genes were identified by assessing the correlation between gene dependency scores from CRISPR knockout screens and *KRAS* mRNA expression in *KRAS*-mutated MSS CRC cell lines in the Cancer Cell Line Encyclopedia (CCLE) database. If the correlation coefficient was ≥ 0.6, the gene was considered a *KRAS* function-sensitive gene. Then *KRAS* function-sensitive genes related to prognosis were screened out in The Cancer Genome Atlas (TCGA) cohort, and the prognostic value was validated in the Gene Expression Omnibus (GEO) cohort. Single-sample gene set enrichment analysis (ssGSEA) was performed to investigate the potential mechanisms. PockDrug-Server was used to predict the druggability of candidate genes. The results showed that in 20 *KRAS*-mutated MSS CRC cell lines, 13 genes were identified as *KRAS* function-sensitive genes. Of these 13 genes, only BIK expression was significantly associated with progression-free survival (PFS) and OS, and the BIK-high patients had significantly poorer PFS (HR=3.18, P=0.020) and OS (HR=4.74, P=0.030) than the BIK-low patients. Multivariate Cox regression analysis revealed high BIK expression as an independent predictor for poorer prognosis in *KRAS*-mutated MSS CRC. The prognostic value of BIK was also successfully validated in a GEO cohort. The results of ssGSEA showed that the BIK-high group was more prone to strong metastasis activity than the BIK-low group. Pocket druggability prediction analysis presented that BIK had three druggable pockets, and their druggability scores were above 0.8. These findings suggested that BIK is a promising prognostic marker and therapeutic target in *KRAS*-mutated MSS CRC.

Keywords: Colorectal cancer, KRAS mutations, microsatellite stable, KRAS function-sensitive genes, BIK

Introduction

According to global cancer statistics in 2018, colorectal cancer (CRC) is the third most often-diagnosed cancer, with its mortality rate ranked second [1]. Microsatellite instability (MSI) and *KRAS* mutation status are among the few biomarkers recommended for routine clinical practice to guide treatment decisions in CRC [2]. According to MSI status, CRC falls into two subtypes: microsatellite stable (MSS) and MSI-high (MSI-H), representing approximately 95% and 5% of all advanced CRC cases, respectively [3]. MSI-H CRC has a better prognosis than MSS CRC [4, 5]. Additionally, MSI-H CRC has higher immune cell infiltration than MSS CRC and shows an excellent response to immunotherapy, leading to the FDA approval of immunotherapy for metastatic MSI-H CRC [6-8].

KRAS is a proto-oncogene encoding a small GTP-binding protein that plays a role in many cellular processes by regulating multiple signaling cascades [9]. *KRAS* mutations are present

in roughly 30%-50% of CRC patients, of which over 95% occur at the hotspots of codons G12, G13, or Q61 [10-12]. It has been well documented that *KRAS* mutations lead to more aggressive tumor biology and shorter overall survival (OS), particularly in MSS metastatic CRC (mCRC), and are a marker for acquired resistance to anti-EGFR therapy [13, 14]. Even with the standard regimen of chemotherapy plus bevacizumab, the prognosis of *KRAS*-mutated MSS mCRC remains poor [15]. Thus, the therapeutic agents against *KRAS*-mutated MSS CRC have been under extensive exploration.

Targeted therapy and immunotherapy are two advanced strategies of cancer treatment. In terms of immunotherapy, recent clinical studies showed that in the *KRAS*-mutated MSS CRC patients, the addition of mono-immunotherapy to chemotherapy plus bevacizumab does not bring significant survival benefits; and the benefit of dual-immunotherapy plus chemotherapy is mediocre, which is similar to that of chemotherapy doublet plus target therapies [16, 17]. Mutant *KRAS* is thought to be an undruggable target due to the lack of hydrophobic pockets for drugs to bind, although approaches for blocking KRAS activity are continually being developed. Current ongoing early-phase clinical trials of the *KRAS* G12C-specific inhibitors, AMG510 and MRTX849, demonstrated encouraging clinical benefit in advanced solid tumors harboring the *KRAS* p.G12C mutation, including CRC [18, 19]. However, in G12 hotspot mutations accounting for around 68% of *KRAS* mutations in mCRC, G12D and G12V are the most frequently observed, with a frequency of about 45% and 31%, respectively, while G12C has a frequency of only 11% [20]. Therefore, identifying novel and effective therapeutic targets is still an urgent clinical need for treating *KRAS*-mutated CRC.

Identifying genes that function closely with *KRAS* and targeting these genes seems to be a promising therapeutic strategy for *KRAS*-mutated MSS CRC. Presently, potential therapeutic targets for *KRAS*-mutated tumors are mainly limited to *KRAS* activation-related genes and its downstream elements. For example, the inhibitors targeting SOS1 and SHP2 interfere with KRAS activation by shifting the equilibrium of KRAS to the GDP-bound state [21, 22]. Clinical trials with several inhibitors of SHP2 and SOS1 (such as TNO155, RMC-4630, JAB-3068, JAB-3312, and BI 1701963) are currently ongoing. Additionally, targeting signaling elements downstream of *KRAS*, such as PI3K/mTOR, mTOR, AKT, and MEK, has shown limited or no improvement in patient survival in clinical trials [23-31]. Undoubtedly, more exhaustive identification of genes associated with *KRAS* function will provide more potential targets.

In this study, we first used *KRAS*-mutated MSS CRC cell lines to screen for *KRAS* function-sensitive genes and then identified the *KRAS* function-sensitive genes with the prognostic value in *KRAS*-mutated MSS CRC cases. We also investigated the potential mechanisms related to prognosis prediction and predicted the druggability of candidate genes.

Materials and methods

Data collection

The proteomic and phosphoproteomic data of *KRAS* and its downstream effectors in *KRAS*-mutated cancer cell lines were collected from a previous study, which provided a proteomic and phosphoproteomic landscape of 43 *KRAS*-mutated cancer cell lines across different tissue origins [32].

The *KRAS* mRNA expression and gene dependency scores in *KRAS*-mutated MSS CRC cell lines were collected from the Cancer Cell Line Encyclopedia (CCLE) https://portals.broadinstitute.org/ccle), a large-scale genomic dataset of human cancer cell lines. CCLE database included 82 CRC cell lines, of which 20 CRC cell lines had MSS phenotype and pathogenic or likely pathogenic *KRAS* mutations. The gene dependency scores were derived from CRISPR knockout screens and reflected the dependency size on a gene by calculating the effect size of knocking out or knocking down a gene [33].

The mRNA expression and clinical data of *KRAS*-mutated CRC patients with stage IV were downloaded from The Cancer Genome Atlas (TCGA) (https://portal.gdc.cancer.gov/) and Gene Expression Omnibus (GEO) (https://www.ncbi.nlm.nih.gov/geo/) database. The TCGA dataset contained 33 *KRAS*-mutated MSS CRC patients. The GEO dataset with the accessing number of GSE104645 consisted of 19 *KRAS*-mutated MSS CRC patients.

A flow chart of this study is shown in Supplementary Figure 1.

Screening for KRAS function-sensitive genes

KRAS function-sensitive genes are those whose functions are sensitive to *KRAS* expression. Here, we defined the *KRAS* function-sensitive gene as the gene whose effects on cell survival after knockout (i.e., gene dependency scores) positively correlate with *KRAS* mRNA expression. As KRAS expression increases, the dependency score of this gene increases, and cell survival is more sensitive to the loss of the protein encoded by this gene. In 20 *KRAS*-mutated MSS CRC cell lines, we investigated the correlation between the dependency scores of 15648 protein-coding genes and *KRAS* mRNA expression, and the genes with correlation coefficients of ≥ 0.6 were recognized as *KRAS* function-sensitive genes.

The prognostic value of KRAS function-sensitive genes

The prognostic value of the *KRAS* function-sensitive genes as continuous variables was initially evaluated in the TCGA cohort to identify the potential genes with prognostic and predictive utility. Then patients were stratified into two groups according to different cut-off values of the mRNA expression of potential prognostic genes identified. The prognostic differences between the two groups were compared via univariate Cox analysis and Kaplan-Meier survival analysis. Multivariate Cox regression analyses evaluated the independent predictive value of the potential prognostic genes regarding progression-free survival (PFS) and OS. The prognostic value was also investigated in the GEO dataset GSE104645, a separate external validation cohort.

Single-sample gene set enrichment analysis

The single-sample gene set enrichment analysis (ssGSEA) is an extension of GSEA and calculates the enrichment scores of every gene set for every sample. We considered the curated pathways with 2,289 gene sets from the Canonical pathways, BioCarta, KEGG, Reactome, and PID. Each ssGSEA enrichment score, reflecting the degree to which the genes in a particular gene set are coordinately up- or down-regulated within a sample, was calculated using the R package "GSVA" and compared between groups using the Wilcoxon rank-sum test. The gene signature was deemed significant if a *P*-value was less than 0.05 and the absolute difference between the mean enrichment scores was over 0.1 in the two groups. The genes in the discovered signature were further analyzed by a web-tool STRING (https://cn.string-db.org/) which estimated the protein-protein interaction networks.

Druggability analysis

PockDrug (http://pockdrug.rpbs.univ-paris-diderot.fr/), as a robust pocket druggability prediction server, was applied to estimate the druggability of candidate genes [34]. The PockDrug-Server provided every pocket with a druggability score between 0 to 1. The pocket with a score of ≥ 0.5 was considered druggable.

Statistical analysis

Differences between groups were evaluated using the Student's t-test or Wilcoxon rank-sum test for continuous variables and the chi-square test or Fisher's exact test for categorical variables. Survival was assessed by non-parametric Kaplan-Meier and semi-parametric Cox proportional hazards analysis. The multivariate Cox proportional hazards model was applied to adjust confounder variables. All *P*-values were reported for the two-tailed test. A *P*-value of less than 0.05 was considered statistically significant unless otherwise specified. All statistical tests were performed using available softwares, packages, and online tools listed in Supplementary Table 1.

Results

The correlation of KRAS mRNA expression with the total and phosphorylated protein levels of KRAS and its downstream effectors

KRAS mutation results in constitutive activation of the KRAS protein, which in turn activates a plethora of phosphorylation signaling pathways, such as the canonical RAF/MEK/ERK pathway, thereby contributing to cancer initiation, progression, and metastasis [35]. Here, we assessed the correlation of *KRAS* mRNA expression obtained from the CCLE database with the KRAS protein and its downstream

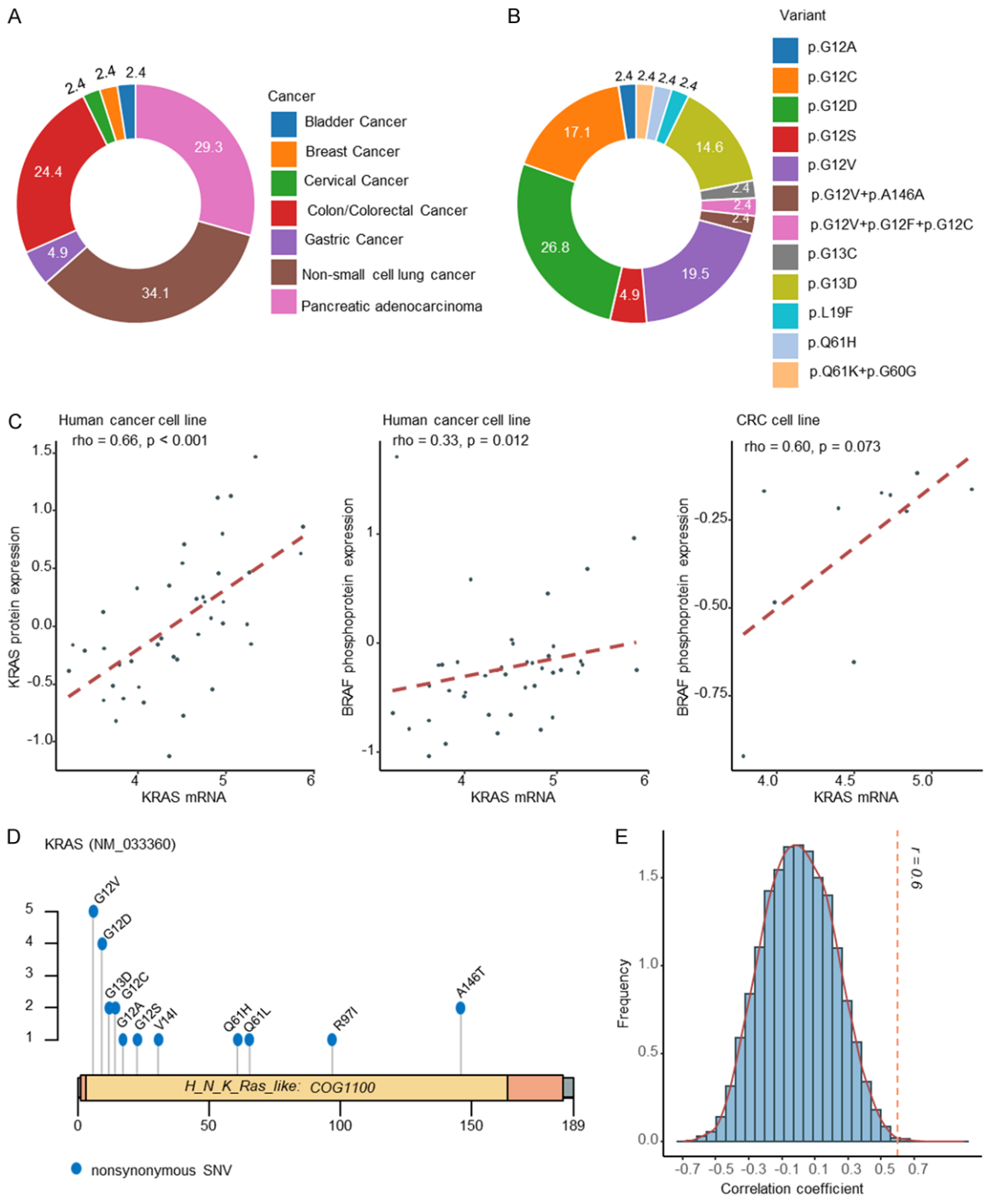

Figure 1. Screening for *KRAS* function-sensitive genes. A. Tissue origin distribution of 41 *KRAS*-mutated human cancer cell lines. B. *KRAS* mutation type distribution of 41 *KRAS*-mutated human cancer cell lines. C. The correlation of *KRAS* mRNA expression with the KRAS protein and its downstream effector BRAF phosphorylation protein levels in *KRAS*-mutated human cancer cell lines. D. Lollipop plot visualizes the location of the entire mutation spots of *KRAS* in 20 *KRAS*-mutated MSS CRC cell lines. E. The distribution of the correlation coefficients between the dependency scores of 15648 genes and KRAS mRNA expression in 20 *KRAS*-mutated MSS CRC cell lines. MSS: Microsatellite Stable; CRC: Colorectal Cancer.

effector BRAF phosphorylation protein level in 41 *KRAS*-mutated human cancer cell lines from a previous study [32]. The tissue origin and mutation sites of these 41 cell lines were shown in **Figure 1A** and **1B**. Non-small cell lung cancer (NSCLC; 14 of 41), pancreatic adenocar-

Table 1. Clinical baseline characteristics of the *KRAS*-mutated MSS CRC patients in the TCGA cohort

Characteristics	Number of patients (N=33)	Patients %
Pathology subtype		
COAD	24	73%
READ	9	27%
Age, median (range)	67 (41-84)	
Sex		
Female	16	48%
Male	17	52%
pT		
T2	1	3%
T3	20	61%
T4	12	36%
pN		
N0	3	9%
N1	13	39%
N2	17	52%
pM		
M1	30	91%
Mx	3	9%

COAD: Colon Adenocarcinoma; READ: Rectum Adenocarcinoma; MSS: Microsatellite Stable; CRC: Colorectal Cancer; TCGA: The Cancer Genome Atlas.

cinoma (PAAD; 12 of 41), and CRC (10 of 41) cell lines were the most common. The most common *KRAS* mutation types were G12D, G12V, G12C, and G13D, accounting for almost 78.0% of all *KRAS* mutations. In these 41 *KRAS*-mutated human cancer cell lines, *KRAS* mRNA expression showed significant positive correlations with KRAS protein (r=0.66, P < 0.001) and phosphorylated BRAF protein level (r=0.33, P=0.012). Additionally, a near-significant correlation (r=0.60, P=0.073) between *KRAS* mRNA expression and phosphorylated BRAF protein level was observed in 10 *KRAS*-mutated CRC cell lines (**Figure 1C**). These findings suggested that in *KRAS*-mutated cancer cell lines, *KRAS* mRNA expression could reflect the activity of KRAS and its downstream effector proteins.

Screening for KRAS function-sensitive genes

Given the above results, we screened *KRAS* function-sensitive genes by exploring the correlation between the gene dependency scores derived from CRISPR knockout screens and *KRAS* mRNA expression in *KRAS*-mutated MSS CRC cell lines. There were 20 *KRAS*-mutated MSS CRC cell lines in the CCLE database. Lollipop plots visualized the entire mutation spots of *KRAS*, wherein G12V was the most common, followed by G12D, G12C, and G13D (**Figure 1D**). The percentage of mutation spots of these cell lines largely reflected the frequency of *KRAS* mutation types in human CRC. The distribution of the correlation coefficients between the dependency scores of 15648 genes and *KRAS* mRNA expression was a bell-shaped curve with a mean of 0.001 (**Figure 1E**). A total of 13 genes with correlation coefficients of ≥ 0.6 were recognized as *KRAS* function-sensitive genes.

The prognostic value of KRAS function-sensitive genes

We first determined the prognostic value of the identified *KRAS* function-sensitive genes as continuous variables in the TCGA cohort, including 33 *KRAS*-mutated MSS CRC patients. The baseline characteristics of the patients in the TCGA cohort are summarized in **Table 1**. Most *KRAS* mutations were G12V (11), G12D (9), G13D (5), and G12C (4), which accounted for 87.9% of all the mutations (**Figure 2A**). In the 13 *KRAS* function-sensitive genes, only BIK mRNA expression analyzed as a continuous variable was significantly associated with PFS (P=0.024) and OS (P=0.011) (Supplementary Table 2). Then discretizing BIK expression using quantiles from 0.1 to 0.9 as cut-off points, we found that the BIK-high group had significantly worse PFS from quantile 0.4 to 0.7 (P < 0.05) and OS from quantile 0.4 to 0.8 (P < 0.05) than the BIK-low group (**Figure 2B** and **2D**). Kaplan-Meier survival curves also showed a significant difference in PFS and OS between the two groups using quantile 0.4 as the cut-off point, wherein the BIK-high group had significantly poorer PFS (P=0.020) and OS (P=0.030) than the BIK-low group (**Figure 2C** and **2E**). These results suggest that interfering with BIK expression to less than 40% may be a rational goal when using BIK as a therapeutic target. Univariate Cox analysis was performed to assess the effects of all baseline characteristics on PFS and OS, and the significant factors (P < 0.1) were then submitted into multivariate Cox

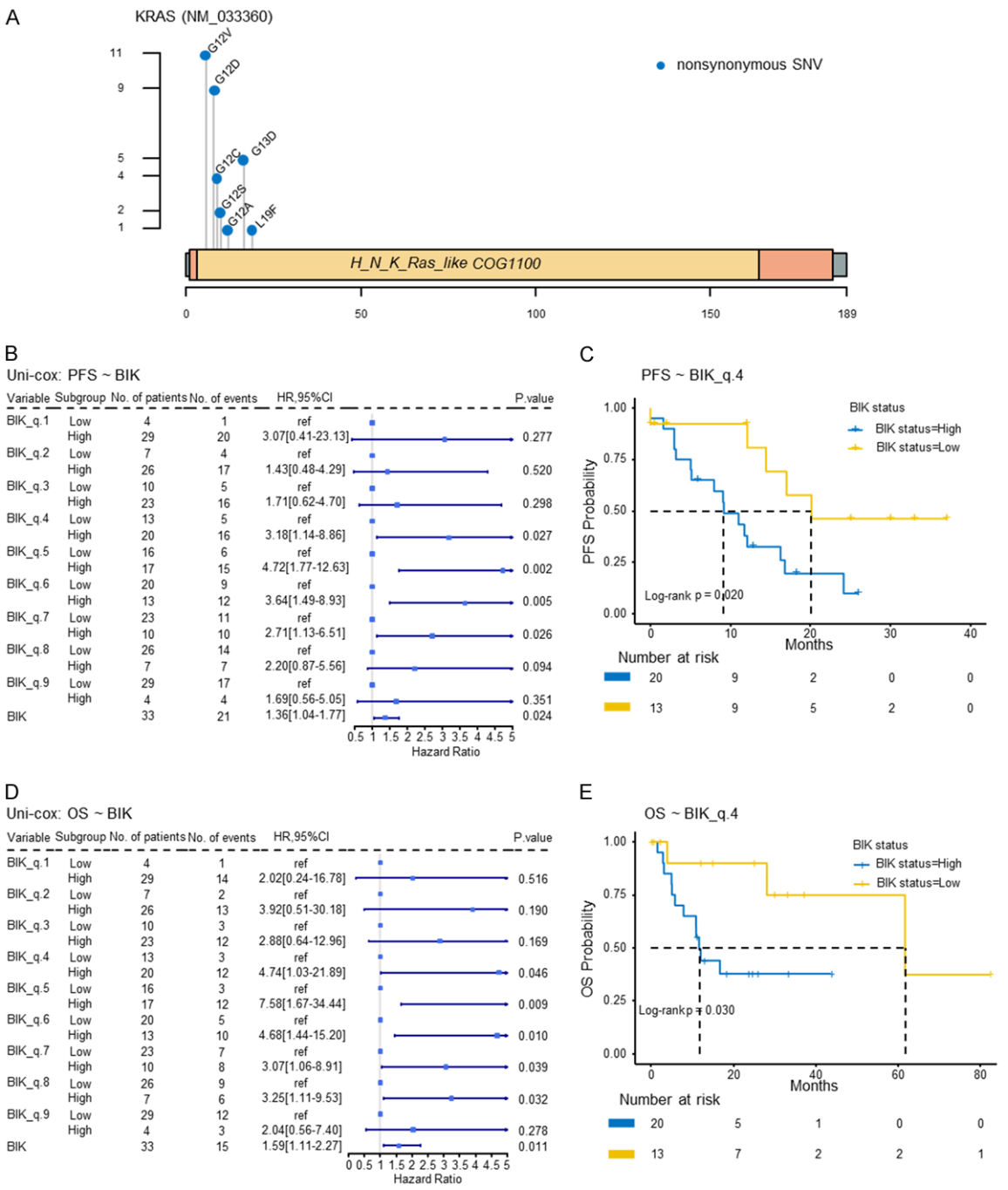

Figure 2. BIK expression is associated with the prognosis of *KRAS*-mutated MSS CRC patients in the TCGA cohort. (A) Lollipop plot visualizes the location of the entire mutation spots of *KRAS* in 33 *KRAS*-mutated MSS CRC patients. (B and D) Univariate Cox regression analyses show that the BIK-high group has significantly worse PFS (B; $P < 0.05$) from quantile 0.4 to 0.7 and OS (D; $P < 0.05$) from quantile 0.4 to 0.8 than the BIK-low group. (C and E) Kaplan-Meier survival curves show a significant difference in PFS (C; P=0.020) and OS (E; P=0.030) between the BIK-high/low groups using quantile 0.4 as the cut-off point. MSS: Microsatellite Stable; CRC: Colorectal Cancer; PFS: Progression-Free Survival; OS: Overall Survival; TCGA: The Cancer Genome Atlas.

regression analysis (**Table 2**). Multivariate Cox regression analysis showed that BIK mRNA expression remained a significant independent predictor of PFS (HR=3.07, 95% CI 1.09-8.65, P=0.034) with a trend toward significance in the independent prediction of OS (HR=4.44, 95% CI 0.93-21.14, P=0.061) (**Figure 3A** and **3B**).

Table 2. Univariate Cox regression analyses of clinical pathological variables against PFS and OS in the TCGA cohort with 33 *KRAS*-mutated MSS CRC patients

Characteristics	Number of patients	PFS			OS		
		Number of events	HR, 95% CI	*P*-value	Number of events	HR, 95% CI	*P*-value
Pathology subtype							
COAD	24	17	ref		14	ref	
READ	9	4	0.45 [0.15-1.35]	0.155	1	0.14 [0.02-1.07]	0.058
Molecular subtype							
CIN	28	18	ref		13	ref	
GS	2	1	0.72 [0.1-5.42]	0.748	1	1.42 [0.18-11.05]	0.738
Sex							
Female	16	8	ref		6	ref	
Male	17	13	0.87 [0.36-2.11]	0.754	9	0.99 [0.35-2.8]	0.985
pN							
N0	3	2	ref		2	ref	
N1	13	8	0.68 [0.14-3.24]	0.627	5	0.34 [0.06-1.82]	0.209
N2	17	11	0.85 [0.19-3.86]	0.829	8	0.52 [0.11-2.49]	0.413
pM							
MX	3	1	ref		0	ref	
M1	30	20	3.26 [0.44-24.39]	0.250	15	\	
Age	33	21	1.01 [0.97-1.05]	0.647	15	1.09 [1.02-1.16]	0.010

COAD: Colon Adenocarcinoma; READ: Rectum Adenocarcinoma; CIN: Chromosomal Instability; GS: Genomic Stable; MSS: Microsatellite Stable; CRC: Colorectal Cancer; TCGA: The Cancer Genome Atlas; PFS: Progression-Free Survival; OS: Overall Survival.

Additionally, the prognostic value of BIK was also investigated in the GEO cohort comprising 19 *KRAS*-mutated MSS CRC patients. The baseline characteristics of this cohort are summarized in **Table 3**. In this cohort, BIK mRNA expression as a continuous variable showed a significant association with PFS (P=0.049) and a near-significant association with OS (P=0.103) (**Figure 3C**).

The mechanism of unfavorable prognosis directed by BIK expression

To investigate the molecular mechanisms underlying the prognostic role of BIK, we conducted the ssGSEA in the BIK-high/low groups in the TCGA cohort. As shown in **Figure 4**, the ssGSEA scores of 13 pathways showed a significant difference between the two groups (adjusted *P* value < 0.2), and all of them were higher in the BIK-low group (**Figure 4A**). It was worth noting that of these 13 pathways, five were integrin-related pathways, which controlled metastasis in various cancers [36-38]. We also analyzed the expression of genes within PID_INTEGRIN_CS_PATHWAY in the two groups. Most genes, including all key node genes, were enriched in the BIK-low group (**Figure 4B**).

Druggability prediction of BIK protein

The druggability of a protein refers to its ability to bind to drug-like molecules with high affinity. Thus, assessing druggability is a necessary first step in discovering new drug targets. Here, we predicted the pocket druggability of BIK protein by the PockDrug-Server and found that BIK had five protein pockets. The parameters of these protein pockets are presented in **Table 4**. Of the five protein pockets, three were druggable pockets with a druggability probability of ≥ 0.5, wherein P2 (0.98, P=0.01) had the highest druggability probability, followed by P1 (0.95, P=0.02) and P0 (0.89, P=0.03). **Figure 5** displayed the BIK protein structure and the potential small molecule binding pockets.

Discussion

KRAS-mutated MSS CRC accounts for about 40% of CRC and has a poor prognosis. Current

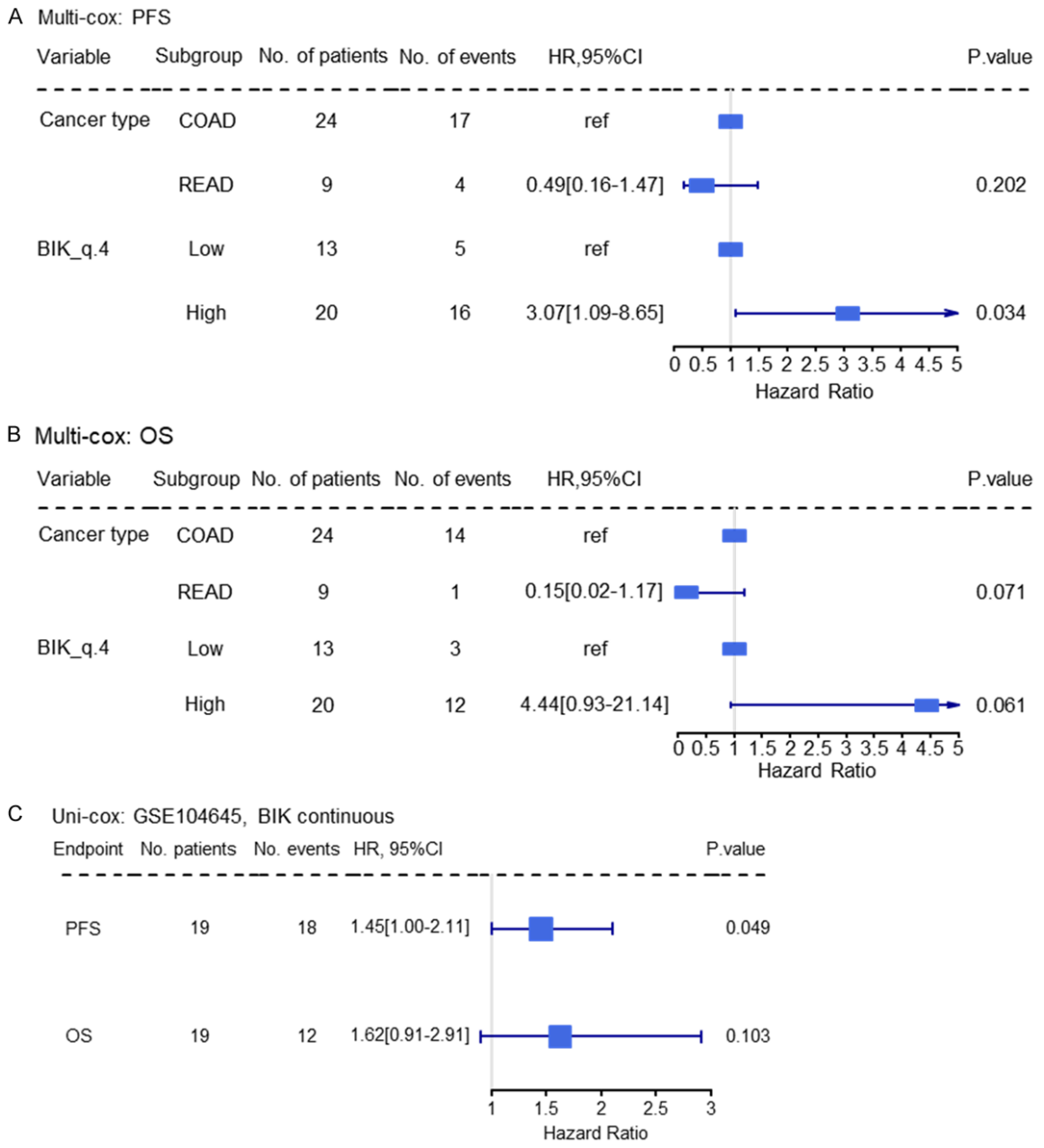

Figure 3. The prognostic value of BIK in the TCGA and GEO cohorts. A and B. Multivariate Cox regression analysis shows that BIK mRNA expression is a significant independent predictor of PFS (P=0.034) with a trend toward significance in the independent prediction of OS (P=0.061). C. BIK mRNA expression as a continuous variable shows a significant association with PFS (P=0.049) and a near-significant association with OS (P=0.061). PFS: Progression-Free Survival; OS: Overall Survival; TCGA: The Cancer Genome Atlas; GEO: Gene Expression Omnibus.

targeted therapeutic drugs, however, are limited. In the present study, we screened *KRAS* function-sensitive genes in *KRAS*-mutated MSS CRC cell lines from the CCLE database and investigated their prognostic and predictive utility in the TCGA cohort. Among 13 identified *KRAS* function-sensitive genes, only BIK mRNA expression was significantly associated with PFS and OS, and high BIK expression was an independent predictor for poor prognosis in *KRAS*-mutated MSS CRC. Besides, the prognostic value of BIK was successfully validated in the GEO cohort. Strong metastasis activity might be a potential mechanism of poor prognosis in BIK-high patients. The pockDrug-Server analysis presented the druggability of three

Table 3. Clinical baseline characteristics of the *KRAS*-mutated MSS CRC patients in the GEO cohort

Characteristics	No. patients	Patients %
Age, median (range)	66 (42-83)	
Sex		
Female	5	26%
Male	14	74%
Primary site		
Ascending	3	16%
Cecum	2	11%
Rectum	8	42%
Sigmoid	6	32%
Number of metastasis		
1	8	42%
2	9	47%
3	2	11%
Molecular subtype		
CMS2	3	16%
CMS3	5	26%
CMS4	11	58%
Chemotherapy		
FOLFIRI	1	5%
FOLFOX	7	37%
FOLFOX + Bev	8	42%
others	1	5%
SOX + Bev	2	11%
Anti-EGFR therapy		
Cetuximab	18	95%
Panitumumab	1	5%

MSS: Microsatellite Stable; CRC: Colorectal Cancer; GEO: Gene Expression Omnibus.

protein pockets of BIK. These results showed that BIK might be a promising prognostic marker and therapeutic target in *KRAS*-mutated MSS CRC.

KRAS mutant cancers have substantial molecular heterogeneity. Tina *et al.* [39] reported that each *KRAS*-mutated cell line has its unique combination of effector dependencies. Even with this heterogeneity, they identified two major subtypes of *KRAS* mutant cancer, either dependent on *RSK* or *KRAS*. Based on the correlation of node dependencies, *RSK*-type lines are closer to wild-type *KRAS* lines than their mutant counterparts in the *KRAS* subtype. Their findings warn against simply comparing *KRAS* mutant with *KRAS* wild-type lines to uncover the complex dependencies of *KRAS* mutant cells. Similarly, the simple comparison of *KRAS* mutant versus *KRAS* wild-type cell lines may not be conducive to identifying *KRAS* function-sensitive genes.

Additionally, we found that in *KRAS*-mutated cancer cell lines, *KRAS* mRNA expression could reflect the activity of KRAS and its downstream effector proteins. Accordingly, a quantitative assessment of the effects of KRAS expression on other molecules will be more helpful in discovering *KRAS* function-sensitive genes. A total of 13 *KRAS* function-sensitive genes were identified in *KRAS*-mutated MSS CRC cell lines. As KRAS expression increased, cell growth inhibition and/or death increased following the knockout of any gene in 13 *KRAS* function-sensitive genes. Given the enormous differences between the *in vivo* and *in vitro* environment, gene expression and function are likely to be dramatically affected. Thus we further investigated the role of *KRAS* function-sensitive genes in *KRAS*-mutated MSS CRC patients, and only BIK was identified as an independent exposure variable whose high expression was associated with a poorer prognosis.

BIK, the first member of the BH3-only proapoptotic proteins, is predominantly localized in the endoplasmic reticulum and induces apoptosis in various eukaryotic cells [40, 41]. It has been reported that BIK acts as a proapoptotic tumor suppressor in several human tissues and plays a suppressive role in tumor progression and metastasis [42-45]. Conversely, BIK was reported to act as an unfavorable prognostic factor in breast cancer. In 2016, Pandya *et al.* [46] analyzed the clinical data of breast cancer patients and identified for the first time BIK as an independent prognostic biomarker for poor outcomes in breast cancer. Subsequently, they performed exhaustive cell experiments to probe the molecular mechanisms of BIK. They analyzed six independent cohorts from public databases to investigate the prognosis value of BIK in estrogen receptor-positive (ER+) breast cancer, the most frequently diagnosed breast cancer subtype. The results showed that BIK drives an aggressive breast cancer phenotype through sublethal apoptosis and predicts poor prognosis in ER-positive breast cancer [47]. As described above, the role of BIK in cancer development is complex, and it may act as a tumor suppressor gene or oncogene depending

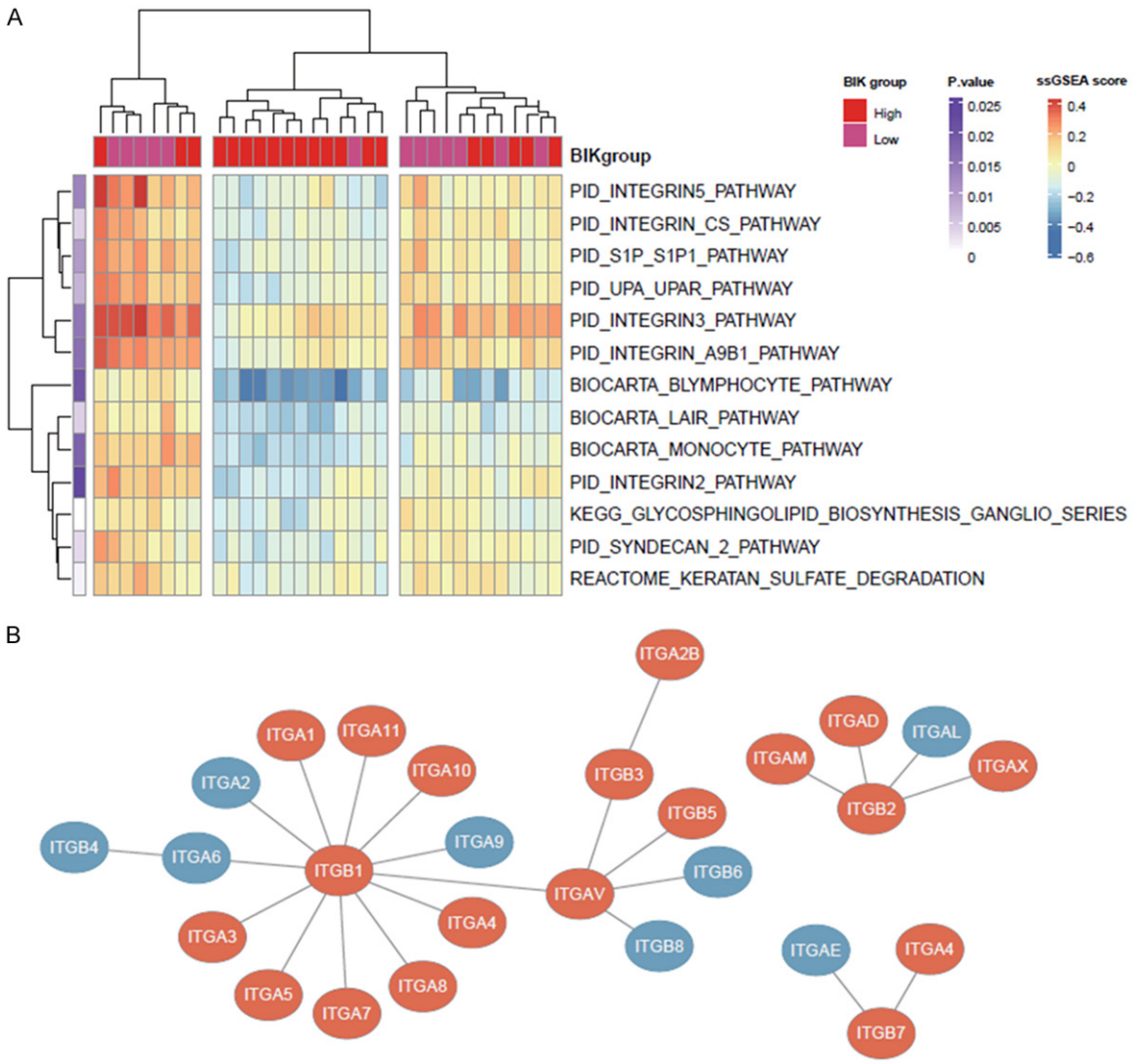

Figure 4. Single-sample gene set enrichment analysis in the TCGA cohort. A. The heatmap of single-sample gene set enrichment analysis of the enriched pathways in the BIK-high/low tumor samples of the TCGA cohort. B. The expression of genes within PID_INTEGRIN_CS_PATHWAY in the BIK-high/low groups. Blue and red circles separately represent down- and upregulated genes in the BIK-low group compared with the BIK-high group. TCGA: The Cancer Genome Atlas.

on the tumor microenvironment. One previous study reported that BIK inhibits cell proliferation, invasion, and migration in two MSS CRC cell lines *in vitro*, one *KRAS* wild-type and the other *KRAS* mutant; however, the role of BIK in tumor initiation and progression in CRC patients has yet to be identified [48]. In this study, we focused on *KRAS*-mutated MSS CRC and identified BIK as an oncogenic factor in *KRAS*-mutated MSS CRC for the first time by analyzing 20 *KRAS*-mutated MSS CRC cell lines and 52 *KRAS*-mutated MSS CRC patients. The results of ssGSEA revealed significant enrichment of integrin-related pathways in the BIK-low samples compared with the BIK-high samples. Integrin-related pathways have been reported to inhibit metastasis in a variety of cancers [36-38]. These findings suggested that the strong metastasis activity might be a contributing factor to a poor prognosis in BIK-high patients. To better understand the underlying molecular mechanisms of the prognostic role of BIK, more experimental studies are clearly required.

The druggability of protein pockets predicts their affinity to bind drug-like molecules and is considered a major criterion for identifying drug

Table 4. The parameters of the five protein pockets in BIK predicted by PockDrug-Server

	Diameter hull	Polar residues	Smallest size	Nlys atom	Ntrp atom	Aromatic residues	Volume hull	Otyr atom	Nb RES	Surface hull	Ooh atom	Hydrophobic kyte	Radius cylinder	Aliphatic residues	Nd1 atom	Hydrophobic residues	Druggability scores
pocket2_atm	11.6	0.5	7.2	0.0	0.0	0.4	256.3	0.0	8.0	224.3	0.0	0.5	5.6	0.1	0.0	0.8	0.98
pocket1_atm	12.6	0.6	6.6	0.0	0.0	0.2	337.5	0.0	9.0	265.4	0.0	0.4	6.0	0.2	0.0	0.7	0.95
pocket0_atm	16.5	0.5	7.6	0.0	0.0	0.2	560.6	0.0	11.0	394.6	0.0	0.2	8.5	0.4	0.0	0.6	0.89
pocket4_atm	13.1	0.6	7.0	0.0	0.0	0.1	348.9	0.0	8.0	282.2	0.0	0.8	6.4	0.3	0.0	0.6	0.31
pocket3_atm	16.1	0.7	7.7	0.0	0.0	0.1	453.5	0.0	10.0	330.3	0.0	2.0	7.9	0.1	0.0	0.5	0.02

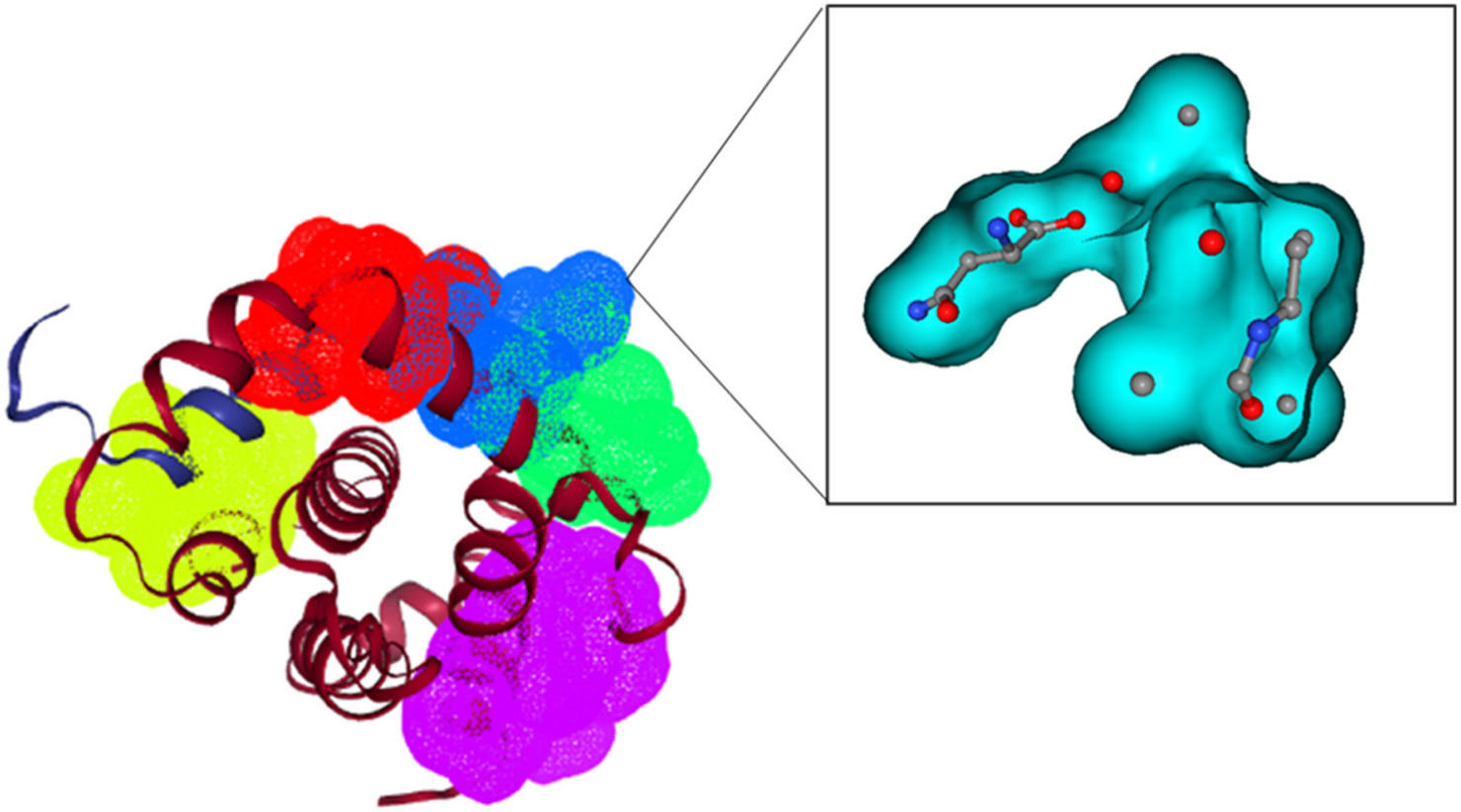

Figure 5. The protein pockets of BIK. Cartoon representation of the BIK protein structure and different protein pockets in BIK according to PockDrug-Server. The box with gray lines represents the enlarged images of the highest-scoring potential small molecule binding pocket (P2).

targets [49]. PockDrug-Server is an online bioinformatics tool for predicting druggability by calculating 66 physicochemical properties of the pockets, such as hydrophobicity, polarity, and aromaticity. The advantage over the recent druggability models for apo pockets is that PockDrug-Server presents consistent results using different pocket estimation methods and is able to distinguish druggable from less druggable pockets clearly [34]. An increasing number of studies adopted PockDrug-Server for druggability predictions [50-54]. Our results showed that BIK had three druggable pockets, and their druggability scores were above 0.8, suggesting that BIK was a promising druggable target for treating *KRAS*-mutated MSS CRC.

This study has some limitations. Firstly, this was a retrospective study based on available data from public datasets, and thus the present results should be viewed as exploratory rather than conclusive. Secondly, the relatively small sample size in the validation cohort restricted our analysis of the prognostic value of BIK, only treating BIK mRNA expression as a continuous variable. Third, the underlying mechanism of the prognostic role of BIK and its potential targeted drugs were not explored deeply. Future research based on *in vitro* and *in vivo* experiments and prospective clinical trials with larger sample sizes is warranted to assess the prognostic value of BIK, dig deep into its mechanisms, validate BIK as a drug target, and develop its potential targeted drugs.

In conclusion, we screened 13 *KRAS* function-sensitive genes by exploring the correlation between the gene dependency score and *KRAS* mRNA expression in *KRAS*-mutated MSS CRC cell lines and identified BIK, one *KRAS* function-sensitive gene, as an independent predictor of prognosis in *KRAS*-mutated MSS CRC patients. Pocket druggability prediction revealed that BIK was a promising druggable target. These findings will contribute to the research on new-targeted therapeutic drugs for *KRAS*-mutated MSS CRC.

Acknowledgements

This study was supported by National Natural Science Foundation of China (No. 82002477).

Disclosure of conflict of interest

None.

Address correspondence to: Dr. Tao Fu, Department of Gastrointestinal Surgery, China-Japan Friendship Hospital, Yinghua Donglu, Heping Jie, Chaoyang District, Beijing 100029, China. Tel: +86-010-64221122; E-mail: Futao916@163.com; Dr. Min Li, Department of Oncology, Nanjing Hospital of Chinese Medicine Affiliated to Nanjing University of Chinese Medicine, No. 157, Daming Road, Qinhuai District, Nanjing 210023, Jiangsu, China. Tel: +86-025-86369114; E-mail: fsyy00340@njucm.edu.cn

References

[1] Bray F, Ferlay J, Soerjomataram I, Siegel RL, Torre LA and Jemal A. Global cancer statistics 2018: GLOBOCAN estimates of incidence and mortality worldwide for 36 cancers in 185 countries. CA Cancer J Clin 2018; 68: 394-424.

[2] Sepulveda AR, Hamilton SR, Allegra CJ, Grody W, Cushman-Vokoun AM, Funkhouser WK, Kopetz SE, Lieu C, Lindor NM and Minsky BD. Molecular biomarkers for the evaluation of colorectal cancer: guideline from the American Society for Clinical Pathology, College of American Pathologists, Association for Molecular Pathology, and American Society of Clinical Oncology. Am J Clin Pathol 2017; 147: 221-260.

[3] Koopman M, Kortman G, Mekenkamp L, Ligtenberg M, Hoogerbrugge N, Antonini N, Punt C and Van Krieken J. Deficient mismatch repair system in patients with sporadic advanced colorectal cancer. Br J Cancer 2009; 100: 266-273.

[4] Greenson JK, Huang SC, Herron C, Moreno V, Bonner JD, Tomsho LP, Ben-Izhak O, Cohen HI, Trougouboff P and Bejhar J. Pathologic predictors of microsatellite instability in colorectal cancer. Am J Surg Pathol 2009; 33: 126.

[5] Popat S, Hubner R and Houlston R. Systematic review of microsatellite instability and colorectal cancer prognosis. J Clin Oncol 2005; 23: 609-618.

[6] Colle R, Cohen R, Cochereau D, Duval A, Lascols O, Lopez-Trabada D, Afchain P, Trouilloud I, Parc Y and Lefevre JH. Immunotherapy and patients treated for cancer with microsatellite instability. Bull Cancer 2017; 104: 42-51.

[7] Le DT, Kim TW, Van Cutsem E, Geva R, Jäger D, Hara H, Burge M, O'Neil B, Kavan P and Yoshino T. Phase II open-label study of pembrolizumab in treatment-refractory, microsatellite instability-high/mismatch repair-deficient metastatic colorectal cancer: KEYNOTE-164. J Clin Oncol 2020; 38: 11.

[8] Andre T, Amonkar M, Norquist JM, Shiu KK, Kim TW, Jensen BV, Jensen LH, Punt CJ, Smith D and Garcia-Carbonero R. Health-related

quality of life in patients with microsatellite instability-high or mismatch repair deficient metastatic colorectal cancer treated with first-line pembrolizumab versus chemotherapy (KEYNOTE-177): an open-label, randomised, phase 3 trial. Lancet Oncol 2021; 22: 665-677.
[9] Pylayeva-Gupta Y, Grabocka E and Bar-Sagi D. RAS oncogenes: weaving a tumorigenic web. Nat Rev Cancer 2011; 11: 761-774.
[10] Tan C and Du X. KRAS mutation testing in metastatic colorectal cancer. World J Gastroenterol 2012; 18: 5171-80.
[11] Dienstmann R, Connor K, Byrne AT, Fridman W, Lambrechts D, Sadanandam A, Trusolino L, Prehn J, Tabernero J and Kolch W. Precision therapy in RAS mutant colorectal cancer. Gastroenterology 2020; 158: 806-811.
[12] Prior IA, Lewis PD and Mattos C. A comprehensive survey of Ras mutations in cancer. Cancer Res 2012; 72: 2457-2467.
[13] Karapetis CS, Khambata-Ford S, Jonker DJ, O'Callaghan CJ, Tu D, Tebbutt NC, Simes RJ, Chalchal H, Shapiro JD and Robitaille S. K-ras mutations and benefit from cetuximab in advanced colorectal cancer. N Engl J Med 2008; 359: 1757-1765.
[14] Taieb J, Le Malicot K, Shi Q, Penault-Llorca F, Bouché O, Tabernero J, Mini E, Goldberg RM, Folprecht G and Luc Van Laethem J. Prognostic value of BRAF and KRAS mutations in MSI and MSS stage III colon cancer. J Natl Cancer Inst 2017; 109: djw272.
[15] Van Cutsem E, Cervantes A, Adam R, Sobrero A, Van Krieken J, Aderka D, Aguilar EA, Bardelli A, Benson A and Bodoky G. ESMO consensus guidelines for the management of patients with metastatic colorectal cancer. Ann Oncol 2016; 27: 1386-1422.
[16] Cremolini C, Rossini D, Antoniotti C, Pietrantonio F, Lonardi S, Salvatore L, Marmorino F, Borelli B, Ambrosini M and Barsotti G. LBA20 FOLFOXIRI plus bevacizumab (bev) plus atezolizumab (atezo) versus FOLFOXIRI plus bev as first-line treatment of unresectable metastatic colorectal cancer (mCRC) patients: results of the phase II randomized AtezoTRIBE study by GONO. Ann Oncol 2021; 32: S1294-S1295.
[17] Ghiringhelli F, Chibaudel B, Taieb J, Bennouna J, Martin-Babau J, Fonck M, Borg C, Cohen R, Thibaudin M and Limagne E. Durvalumab and tremelimumab in combination with FOLFOX in patients with RAS-mutated, microsatellite-stable, previously untreated metastatic colorectal cancer (MCRC): results of the first intermediate analysis of the phase Ib/II MEDETREME trial. J Clin Oncol 2020; 38: 3006.
[18] Hong DS, Fakih MG, Strickler JH, Desai J, Durm GA, Shapiro GI, Falchook GS, Price TJ, Sacher A and Denlinger CS. KRASG12C inhibition with sotorasib in advanced solid tumors. N Engl J Med 2020; 383: 1207-1217.
[19] Hallin J, Engstrom LD, Hargis L, Calinisan A, Aranda R, Briere DM, Sudhakar N, Bowcut V, Baer BR and Ballard JA. The KRASG12C inhibitor MRTX849 provides insight toward therapeutic susceptibility of KRAS-mutant cancers in mouse models and patients. Cancer Discov 2020; 10: 54-71.
[20] Patelli G, Tosi F, Amatu A, Mauri G, Curaba A, Patanè D, Pani A, Scaglione F, Siena S and Sartore-Bianchi A. Strategies to tackle RAS-mutated metastatic colorectal cancer. ESMO open 2021; 6: 100156.
[21] Nichols RJ, Haderk F, Stahlhut C, Schulze CJ, Hemmati G, Wildes D, Tzitzilonis C, Mordec K, Marquez A and Romero J. RAS nucleotide cycling underlies the SHP2 phosphatase dependence of mutant BRAF-, NF1-and RAS-driven cancers. Nat Cell Biol 2018; 20: 1064-1073.
[22] Hofmann MH, Gmachl M, Ramharter J, Savarese F, Gerlach D, Marszalek JR, Sanderson MP, Kessler D, Trapani F and Arnhof H. Bi-3406, a potent and selective sos1-kras interaction inhibitor, is effective in kras-driven cancers through combined mek inhibition. Cancer Discov 2021; 11: 142-157.
[23] Carlo MI, Molina AM, Lakhman Y, Patil S, Woo K, DeLuca J, Lee CH, Hsieh JJ, Feldman DR, Motzer RJ and Voss MH. A phase Ib study of BEZ235, a dual inhibitor of phosphatidylinositol 3-kinase (PI3K) and mammalian target of rapamycin (mTOR), in patients with advanced renal cell carcinoma. Oncologist 2016; 21: 787-788.
[24] Blumenschein G Jr, Smit E, Planchard D, Kim DW, Cadranel J, De Pas T, Dunphy F, Udud K, Ahn MJ and Hanna N. A randomized phase II study of the MEK1/MEK2 inhibitor trametinib (GSK1120212) compared with docetaxel in KRAS-mutant advanced non-small-cell lung cancer (NSCLC). Ann Oncol 2015; 26: 894-901.
[25] Salazar R, Garcia-Carbonero R, Libutti SK, Hendifar AE, Custodio A, Guimbaud R, Lombard-Bohas C, Ricci S, Klümpen HJ and Capdevila J. Phase II study of BEZ235 versus everolimus in patients with mammalian target of rapamycin inhibitor-naïve advanced pancreatic neuroendocrine tumors. Oncologist 2018; 23: 766-e790.
[26] Ng K, Tabernero J, Hwang J, Bajetta E, Sharma S, Del Prete SA, Arrowsmith ER, Ryan DP, Sedova M and Jin J. Phase II study of everolimus in patients with metastatic colorectal adenocarcinoma previously treated with bevacizumab-, fluoropyrimidine-, oxaliplatin-, and irinote-

can-based regimens. Clin Cancer Res 2013; 19: 3987-3995.
[27] Spindler KL, Sorensen MM, Pallisgaard N, Andersen RF, Havelund BM, Ploen J, Lassen U and Jakobsen AK. Phase II trial of temsirolimus alone and in combination with irinotecan for KRAS mutant metastatic colorectal cancer: outcome and results of KRAS mutational analysis in plasma. Acta Oncol 2013; 52: 963-970.
[28] Samalin E, Fouchardière C, Thézenas S, Boige V, Senellart H, Guimbaud R, Taïeb J, François E, Galais MP, Lièvre A, Seitz JF, Metges JP, Bouché O, Boissière-Michot F, Lopez-Crapez E, Bibeau F, Ho-Pun-Cheung A, Ychou M, Adenis A, Di Fiore F and Mazard T. Sorafenib plus irinotecan combination in patients with RAS-mutated metastatic colorectal cancer refractory to standard combined chemotherapies: a multicenter, randomized phase 2 trial (NEXIRI-2/PRODIGE 27). Clin Colorectal Cancer 2020; 19: 301-310, e301.
[29] Yap TA, Yan L, Patnaik A, Fearen I, Olmos D, Papadopoulos K, Baird RD, Delgado L, Taylor A, Lupinacci L, Riisnaes R, Pope LL, Heaton SP, Thomas G, Garrett MD, Sullivan DM, de Bono JS and Tolcher AW. First-in-man clinical trial of the oral pan-AKT inhibitor MK-2206 in patients with advanced solid tumors. J Clin Oncol 2011; 29: 4688-95.
[30] Brana I, Berger R, Golan T, Haluska P, Edenfield J, Fiorica J, Stephenson J, Martin L, Westin S and Hanjani P. A parallel-arm phase I trial of the humanised anti-IGF-1R antibody dalotuzumab in combination with the AKT inhibitor MK-2206, the mTOR inhibitor ridaforolimus, or the NOTCH inhibitor MK-0752, in patients with advanced solid tumours. Br J Cancer 2014; 111: 1932-1944.
[31] Wisinski KB, Tevaarwerk AJ, Burkard ME, Rampurwala M, Eickhoff J, Bell MC, Kolesar JM, Flynn C and Liu G. Phase I study of an AKT inhibitor (MK-2206) combined with lapatinib in adult solid tumors followed by dose expansion in advanced HER2+ breast cancer. Clin Cancer Res 2016; 22: 2659-2667.
[32] Liu Z, Liu Y, Qian L, Jiang S, Gai X, Ye S, Chen Y, Wang X, Zhai L and Xu J. A proteomic and phosphoproteomic landscape of KRAS mutant cancers identifies combination therapies. Mol Cell 2021; 81: 4076-4090, e4078.
[33] Meyers RM, Bryan JG, McFarland JM, Weir BA, Sizemore AE, Xu H, Dharia NV, Montgomery PG, Cowley GS and Pantel S. Computational correction of copy number effect improves specificity of CRISPR-Cas9 essentiality screens in cancer cells. Nat Genet 2017; 49: 1779-1784.
[34] Hussein HA, Borrel A, Geneix C, Petitjean M, Regad L and Camproux AC. PockDrug-Server: a new web server for predicting pocket druggability on holo and apo proteins. Nucleic Acids Res 2015; 43: W436-W442.
[35] Ryan MB and Corcoran RB. Therapeutic strategies to target RAS-mutant cancers. Nat Rev Clin Oncol 2018; 15: 709-720.
[36] Felding-Habermann B. Integrin adhesion receptors in tumor metastasis. Clin Exp Metastasis 2003; 20: 203-213.
[37] Ramsay AG, Marshall JF and Hart IR. Integrin trafficking and its role in cancer metastasis. Cancer Metastasis Rev 2007; 26: 567-578.
[38] Hamidi H and Ivaska J. Every step of the way: integrins in cancer progression and metastasis. Nat Rev Cancer 2018; 18: 533-548.
[39] Yuan TL, Amzallag A, Bagni R, Yi M, Afghani S, Burgan W, Fer N, Strathern LA, Powell K and Smith B. Differential effector engagement by oncogenic KRAS. Cell Rep 2018; 22: 1889-1902.
[40] Chinnadurai G, Vijayalingam S and Rashmi R. BIK, the founding member of the BH3-only family proteins: mechanisms of cell death and role in cancer and pathogenic processes. Oncogene 2008; 27: S20-S29.
[41] Chinnadurai G, Vijayalingam S and Gibson SB. BNIP3 subfamily BH3-only proteins: mitochondrial stress sensors in normal and pathological functions. Oncogene 2008; 27: S114-S127.
[42] Zhang L, Li X, Chao Y, He R, Liu J, Yuan Y, Zhao W, Han C and Song X. KLF4, a miR-32-5p targeted gene, promotes cisplatin-induced apoptosis by upregulating BIK expression in prostate cancer. Cell Commun Signal 2018; 16: 1-11.
[43] Yuan C, Ding Y, Zhuang Y, Zhang C, Han L, Li W, Guo R and Zhang E. Copy number amplification-activated long non-coding RNA LINC00662 epigenetically inhibits BIK by interacting with EZH2 to regulate tumorigenesis in non-small cell lung cancer. J Cancer 2022; 13: 1640-1651.
[44] Zhang L, Li X, Chao Y, He R, Liu J, Yuan Y, Zhao W, Han C and Song X. KLF4, a miR-32-5p targeted gene, promotes cisplatin-induced apoptosis by upregulating BIK expression in prostate cancer. Cell Commun Signal 2018; 16: 53.
[45] Borst A, Haferkamp S, Grimm J, Rösch M, Zhu G, Guo S, Li C, Gao T, Meierjohann S, Schrama D and Houben R. BIK is involved in BRAF/MEK inhibitor induced apoptosis in melanoma cell lines. Cancer Lett 2017; 404: 70-78.
[46] Pandya V, Glubrecht D, Vos L, Hanson J, Damaraju S, Mackey J, Hugh J and Goping S. The pro-apoptotic paradox: the BH3-only protein Bcl-2 interacting killer (Bik) is prognostic for unfavorable outcomes in breast cancer. Oncotarget 2016; 7: 33272.

[47] Pandya V, Githaka JM, Patel N, Veldhoen R, Hugh J, Damaraju S, McMullen T, Mackey J and Goping IS. BIK drives an aggressive breast cancer phenotype through sublethal apoptosis and predicts poor prognosis of ER-positive breast cancer. Cell Death Dis 2020; 11: 1-19.

[48] Feng L, Jing L, Han J, Wang G, Liu Y, Zhang X, Wang Y, Wang F, Ma H and Liu Y. MicroRNA 486-3p directly targets BIK and regulates apoptosis and invasion in colorectal cancer cells. Onco Targets Ther 2018; 11: 8791.

[49] Abi Hussein H, Geneix C, Petitjean M, Borrel A, Flatters D and Camproux AC. Global vision of druggability issues: applications and perspectives. Drug Discovery Today 2017; 22: 404-415.

[50] Hamza M, Ali A, Khan S, Ahmed S, Attique Z, Ur Rehman S, Khan A, Ali H, Rizwan M and Munir A. NCOV-19 peptides mass fingerprinting identification, binding, and blocking of inhibitors flavonoids and anthraquinone of Moringa oleifera and hydroxychloroquine. J Biomol Struct Dyn 2021; 39: 4089-4099.

[51] Siddiqa MA, Rao D, Suvarna G, Chennamachetty V, Verma M and Rao M. In-silico drug designing of spike receptor with its ACE2 receptor and Nsp10/Nsp16 mtase complex against SARS-CoV-2. Int J Pept Res Ther 2021; 27: 1633-1640.

[52] Teixeira O, Lacerda P, Froes TQ, Nonato MC and Castilho MS. Druggable hot spots in trypanothione reductase: novel insights and opportunities for drug discovery revealed by DRUGpy. J Comput Aided Mol Des 2021; 35: 871-882.

[53] Yang YF, Yu B, Zhang XX and Zhu YH. Identification of TNIK as a novel potential drug target in thyroid cancer based on protein druggability prediction. Medicine 2021; 100: e25541.

[54] Kefala Stavridi A, Appleby R, Liang S, Blundell TL and Chaplin AK. Druggable binding sites in the multicomponent assemblies that characterise DNA double-strand-break repair through non-homologous end joining. Essays Biochem 2020; 64: 791-806.

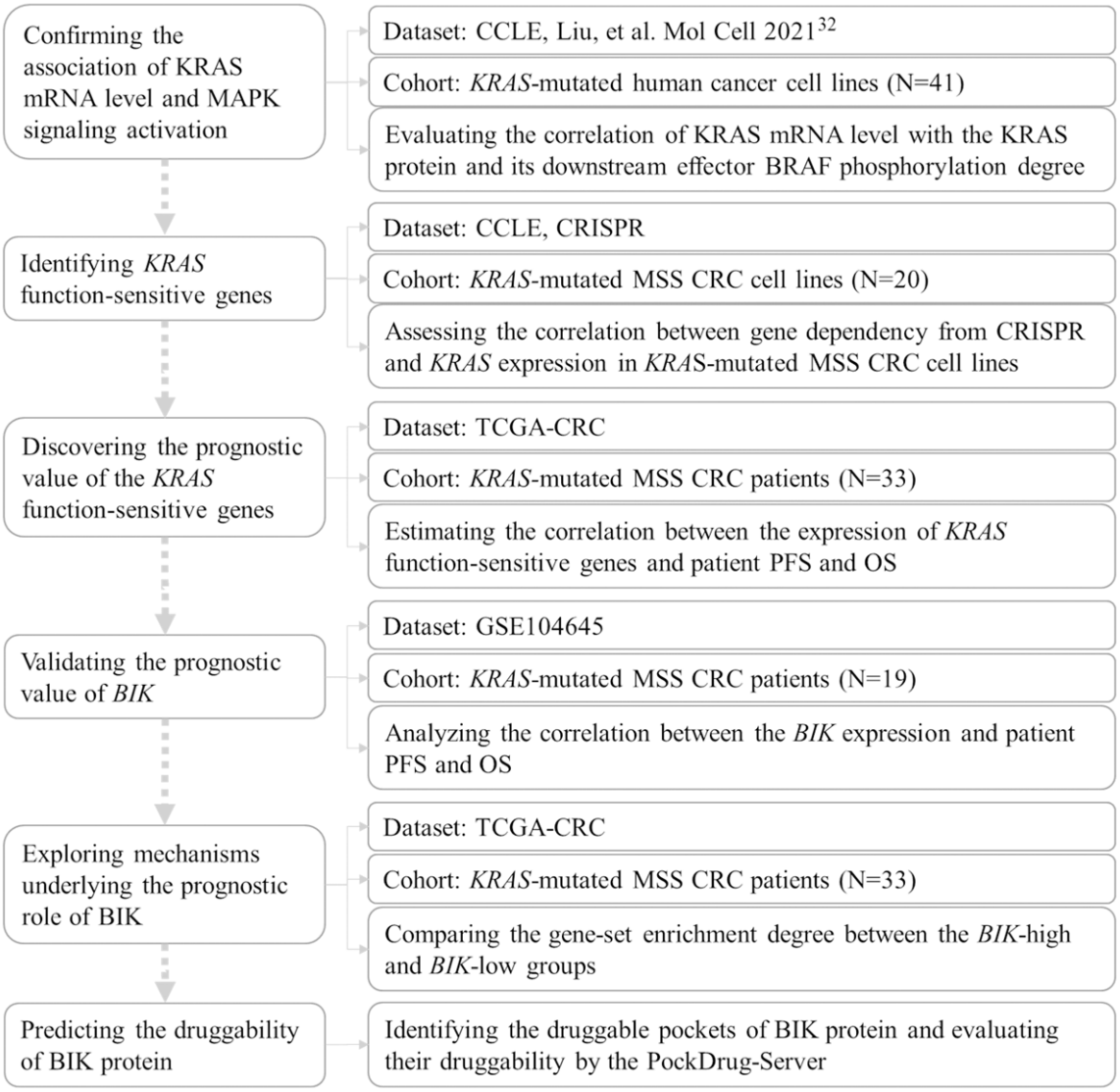

Supplementary Figure 1. Study flow chart. CCLE: Cancer Cell Line Encyclopedia; MSS: Microsatellite Stable; CRC: Colorectal Cancer; PFS: Progression-Free Survival; OS: Overall Survival; TCGA: The Cancer Genome Atlas.

Supplementary Table 1. List of softwares, packages, and online tools used for this study

Name	Type	Version number or URL	Purpose
Python	software	3.9.5	General data analysis
R	software	4.2.0	Data analysis and visulazation
survival	R package	3.4.0	Survival analysis
survminer	R package	0.4.9	Survival analysis
GSVA	R package	1.44.5	ssGSEA
maftools	R package	2.12.0	Lollipop plot
pheatmap	R package	1.0.12	Heatmap plot
forestplot	R package	2.0.1	Forest plot
Cytoscape	software	3.9.1	Pathway visualization
STRING	Online tool	https://cn.string-db.org/	Protein-protein interation estimation
PockDrug	Online tool	http://pockdrug.rpbs.univ-paris-diderot.fr/cgi-bin/index.py?page=home	Pocket and druggability prediction

ssGSEA: Single-Sample Gene Set Enrichment Analysis.

Supplementary Table 2. Univariate Cox regression analyses of the expression of 11 *KRAS* function-sensitive genes as continuous variables against PFS and OS in the TCGA cohort with 33 *KRAS*-mutated MSS CRC patients

Gene symbol	PFS		OS	
	HR, 95% CI	*P* value	HR, 95% CI	*P* value
BIK	1.36 [1.04-1.77]	0.024	1.59 [1.11-2.27]	0.011
C3orf17	0.99 [0.7-1.4]	0.954	1.01 [0.69-1.48]	0.956
CAPNS2	0.91 [0.76-1.08]	0.269	0.84 [0.68-1.04]	0.118
CHST6	0.98 [0.79-1.22]	0.883	0.96 [0.73-1.27]	0.777
DAPK3	1.22 [0.8-1.84]	0.353	1.31 [0.79-2.15]	0.294
GIPC2	0.95 [0.74-1.2]	0.656	1.0 [0.71-1.4]	0.995
GOLGA7	0.92 [0.68-1.23]	0.577	0.84 [0.6-1.18]	0.307
HEATR5B	0.89 [0.55-1.42]	0.619	0.64 [0.37-1.11]	0.113
IRX3	1.02 [0.82-1.26]	0.866	1.06 [0.83-1.36]	0.623
PLK4	0.93 [0.65-1.32]	0.674	0.97 [0.62-1.5]	0.879
SLC9A4	1.06 [0.86-1.3]	0.605	1.05 [0.83-1.34]	0.684

Note: 2 genes are removed: FREM3 is not found in TCGA, nor does its alias; SYCN expression is not available in all samples. PFS: Progression-Free Survival; OS: Overall Survival; MSS: Microsatellite Stable; CRC: Colorectal Cancer; TCGA: The Cancer Genome Atlas.